RSC Advances




ROYAL SOCIETY OF CHEMISTRY

www.rsc.org/advances

RSC Advances

ARTICLE

# Safflomin A inhibit neuraminidase activity and influenza virus replication

Miao Yu[a], Ye Wang[b], Li Tian[c], Yanyan Wang[a], Xizhu Wang[a], Weiguo Liang[a], Jiyu Yang[a], Dahai Yu[a], Tonghui Ma[d*], Xuexun Fang[a*]

Received 00th January 20xx,
Accepted 00th January 20xx

DOI: 10.1039/x0xx00000x

www.rsc.org/

Neuraminidase (NA) is a glycoprotein on the surface of influenza virus that plays an important role in early process of virus infection and viral release from the infected cells. NA inhibitors are currently the most effective drugs to treat influenza virus infection. Many traditional Chinese medicines (TCMs) in various formulations have been used in the Chinese clinics to treat influenza, however, the effective constituents and the mechanism of action are mostly unknown. In this paper, we have tested almost 300 natural compounds from a Chinese medicinal herbal compound library to evaluate their anti-NA activities in *vitro*. Safflomin A (SA) was one of the compound detected with NA inhibitory activities. It showed inhibition against neuraminidases from H1N1 and H3N2 of type A and neuraminidase of type B influenza virus. Enzyme kinetic tests using SA revealed that the type of inhibition against N1 and N2 neuraminidases were noncompetitive. The interaction of SA with the N1 and N2 neuraminidases was analyzed using molecular simulation and docking, which showed that SA bound in the non-active site of N1 and N2. SA was also analyzed for its cytotoxicity and its anti-viral activities in cell culture. It showed inhibitory effect for viral replication of H1N1 and H3N2 influenza virus in MDCK cells. Enzymatic analysis indicated that SA and oseltamivir carboxylate combination treatment was synergistic with combination index (CI) values ranging between 0.49 and 0.52 against neuraminidase of A/New Caledonia/20/1999 (H1N1), and ranging between 0.56 and 0.88 against neuraminidase of A/Fujian/411/2002 (H3N2). These results suggest that an herbal formulation containing SA in combination with oseltamivir carboxylate may serve as a potential therapeutic option to currently available anti-influenza therapeutics.

## Introduction

Influenza virus annually cause epidemic and complications, and even significant morbidity and fatality, especially in the senior citizens who have underlying cardiopulmonary diseases.[1, 2] In 2009, worldwide H1N1 influenza epidemics infected millions and caused severe fatality. In February 2013, a novel avian influenza H7N9 virus merged in China and was found to infect humans.[3] There is evidence that influenza pandemics occurred four times in the 20th century and caused 20 to 50 million deaths worldwide.[4] Influenza like symptoms typically include headache, sore throat, muscle ache, fatigue and fever. Most patients were critically ill and presented sever pneumonia, acute kidney failure, acute respiratory distress syndrome, diffuse intravascular coagulation and septic shock.[4-6]

Influenza virus is a highly infectious respiratory virus which could infect human and other animals and is classified into three genera (i.e. influenza A, B and C).[7] There are two different types of viral integral glycoproteins, named hemagglutinin (HA) and neuraminidase (NA). The influenza A

[a] *Key Laboratory for Molecular Enzymology and Engineering of Ministry of Education, College of Life Sciences, Jilin University, 2699 Qianjin Street, Changchun 130012, China.*
[b] *School of Life Science, Jilin University, 2699 Qianjin Street Changchun 130012, China.*
[c] *State Key Laboratory of Electroanalytical Chemistry, Changchun Institute of Applied Chemistry, Chinese Academy of Sciences, Changchun 130022, China.*
[d] *College of Basic Medical Sciences, Dalian Medical University, Dalian 116000, China.*

[*] *Corresponding author: Xuexun Fang. Key Laboratory for Molecular Enzymology and Engineering of Ministry of Education, Jilin University, 2699 Qianjin Street Changchun 130012, China; Tel. and fax: +86-431-85155249; E-mail address: fangxx@ jlu.edu.cn*
*Tonghui Ma. College of Basic Medical Sciences, Dalian Medical University, Dalian 116000, China; Tel. and fax: +86-0411-86110378; E-mail address: tonghuima@dlmedu.edu.cn*

† Footnotes relating to the title and/or authors should appear here.
Electronic Supplementary Information (ESI) available: [details of any supplementary information available should be included here]. See DOI: 10.1039/x0xx00000x

virus is called by the type of HA (H1-H16) and NA (N1-N9) it contains. The structure of the two proteins change easily through a process of antigenic drift that could result in influenza virus variations. According to the "150-cavity" adjacent to the active site, the NA of influenza A has been divided into two different classes, known as group-1 (comprising N1, N4, N5, N8) and group-2 (comprising N2, N3, N6, N7, N9).[8] The NA plays an important role in influenza A virus replication and facilitates the early process of influenza virus infection in human airway epithelium, which can cleave terminal sialic acids of sialoglycans and promote the release of progeny virus from the infected host cell.[7-10] Hence, as an ideal target for design of anti-influenza drugs, the NA presents on the surface of the influenza virus has attracted global attention.

Since vaccination is less effective or not available upon the influenza virus variants outbreak, the primary focus of attention has been on drugs. There are only two classes of anti-influenza drugs approved by U.S. FDA for the clinical treatment and prophylaxis: M2 ion channel blockers (Amantadine and Rimantadine) and neuraminidase inhibitors (Oseltamivir, Zanamivir and Peramivir). According to the U.S. Centers for Disease Control and Prevention, 100% of seasonal H3N2 and 2009 pandemic flu have shown resistance to adamantanes and rimantadine, thus amantadine and rimantadine are no longer recommended for treatment of influenza.[11] The neuraminidase inhibitors are currently the only clinically effective drugs to treat influenza. However, all of these synthetic drugs have the side effects and the widely used of these drugs resulted in the emergence of drug-resistant mutant viruses in recent years.[12-14] Studies have shown that influenza virus isolated in human resistant to oseltamivir were frequent in Japan than in Europe.[15] There were 20% isolates in Europe which was oseltamivir-resistant H1N1 mutants.[16] Influenza viruses which has resistant have universal shape of the NA catalytic site. The active site of the NA content 8 functional residues (R118, D151, R152, R224, E276, R292, R371 and Y406) and surrounded by 11 framework residues (E119, R156, W178, S179, D198, I222, E227, H274, E277, N294 and E425).[17] Both oseltamivir and zanamivir inhibited NA by competing with the substrate at the catalytic site. One single change of catalytic site of NA could reduce the inhibition of oseltamivir or zanamivir to the influenza virus. H274Y mutation of influenza virus (H1N1) was reported to be oseltamivir resistant.[18] Vasiliy P. *et al*. found neuraminidase D151G mutation of influenza A (H3N2) was more resistant to the zanamivir and the $IC_{50}$ was almost increased 1500-fold.[19] In recent years, the novel avian H7N9 caused more than 227 deaths in the world. This novel H7N9 virus is a triple reassortant virus taking along genes from H7N3, H9N2 and H11N9 or H2N9 avian influenza A viruses.[20] Zhou *et al*. found that the H7N9 virus can bind to both avian-type and human-type receptors.[21] The isolated H7N9 with neuraminidase R292K mutation is broad resistance to neuraminidase inhibitors.[20, 22] Due to lack of the commercial drugs and emergence of oseltamivir-resistant virus, new drugs should be presented to oppose this new fatal influenza virus.

Favipiravir (T-705) is an antiviral drug that selectively inhibits the RNA-dependent RNA polymerase of influenza virus.[21] Sleeman et al. found that favipiravir inhibits in vitro replication of a wide range of influenza viruses, including those resistant to currently available drugs.[23] Other interesting drug targets, such as nucleoprotein, viral polymerase, and non-structural protein NS1A, have recently been well reviewed by Das and colleagues.[24] In 2009, Dias et al. showed that a intrinsic RNA and DNA endonuclease is located in the PA subunit of virus polymerase. Inhibitors targeting of this endonuclease may also emerge as potential new anti-influenza drugs.[25]

Herbal remedies with the natural and active substances play a role as anti-influenza agents in controlling and treatment of influenza virus. A series of traditional Chinese medicinal (TCM) has been reported with antiviral effects, such as *Melia toosendan* could inhibit influenza virus through suppression of NA both in *vitro* and *vivo*.[26] *Forsythia suspensa* extract against influenza A virus (H1N1) in *vitro* and in *vivo* using the cytopathic effect and Neutral Red dye uptake assays.[27] Based on a large amount of studies, a variety of efficiently bioactive compounds isolated from TCMs have been identified to treat influenza.[7] In the last few years, researchers had focused on the components of herbs to anti-influenza. Jin-Yuan Ho *et al*. extracted the ethanolic component from *Paeonia lactiflora*, which exhibited low $IC_{50}$ values against influenza virus A/WSN/33 (H1N1) in *vitro* and *vivo*. It also has inhibitory activity against H1N1pdm strain which was isolated from clinical oseltamivir-resistant virus.[28] The aqueous extracts of *H. erectum*, *M cochinchinensis* and *T. chebula* reduced the titre of A/Teal/Tunka/7/2010 (H3N8) in *vitro*.[29] Wang *et al*. used a system pharmacology approach to detect 50 compounds from two herbs aim to map to target-disease and drug-target-pathway networks in *silico*.[30]

Computer-based modeling methodology has been widely used to design new drugs. It enhanced efficiency of detection and reduced the cost of experiment. Molecular docking has been usually utilized to drug discovery especially against influenza virus.[31] An *et al*. utilized computational molecular docking to identify potential inhibitors of the H5N1 NA in 20 compounds.[32] Tambunan *et al*. found two ligands that have good $IC_{50}$ values of the target interaction to H1N1 NA and toxicological properties using simulation results of molecular docking. These two ligands are predicted with no mutagencity or carcinogenicity and have good oral bioavailability.[33] We have also taken advantage of homology modeling to simulate the structure of H1N1 NA, the model structure of N1 was used to screen compounds of NPD database [34] for potential inhibitors. We found 34 of compounds with low affinity energy, among which, two natural compounds (ZINC02128091 and ZINC02098378) possessed the most favorable interaction energy.[35]

In this study, we tested 289 natural compounds by NA inhibition assay. Among these compounds, safflomin A (SA) showed NA inhibitory activity and was analyzed for its anti-

viral effect by measuring cytopathic effect (CPE) of the influenza A virus. We also determined the type of inhibition of SA towards NA by enzyme kinetics. Moreover, the interaction of SA and influenza NA was analyzed by molecular docking. Finally, combination studies were undertaken to investigate whether SA could act synergistically with oseltamivir carboxylate against the NA of H1N1 and H3N2.

## Materials and methods

### 2.1 Reagents

2-(N-morpholino) ethanesulfonic acid (MES, >99%), dimethylsulfoxide (DMSO), 2'-(4-methylumbelliferyl)-α-D-N-acetylneuraminic acid, sodium salt hydrate (MU-NANA, CAS No. M8639) and 3-[4,5-dimethyl-thiazol-2-yl]-2,5- diphenyl tetrazolium bromide (MTT, >98%) were purchased from Sigma-Aldrich Corporation. Fetal bovine serum (FBS), Dulbecco's modified Eagle's medium (DMEM), TPCK-treated trypsin and Trypsin-EDTA were purchased from the Gibco Company. Oseltamivir carboxylate was purchased from Dalian meilun biology technology co.. Other chemical reagents were purchased from Beijing Chemical Works.

### 2.2 Compounds from traditional Chinese medicines (TCMs)

All compounds (analytical reagent, see Appendix) which are ingredients of TCMs were purchased from the Chinese Standard Chemical Networks (http://www.crmrm.com/) Each compound was dissolved in DMSO to the final concentration of 20 mM and stored in 96-well plates numbered α, β, γ, and δ at -80 ℃.

### 2.3 Cells and virus

Madin-Darby canine kidney (MDCK) cells were obtained from Norman Bethune Health Science Center of Jilin University and grown in DMEM supplemented with 10% FBS, 100 μg/mL streptomycin, 100 U/mL penicilin. Influenza viruses (A/New Caledonia/20/1999 (H1N1), A/Fujian/411/2002 (H3N2), B/Jiangsu/10/2003) which were used as the source of NAs was obtained from Changchun Institute of Biological Products. Each type was propagated in 9-days old embryonated chicken eggs. The allantoic fluid was collected, then centrifuged at 3000 rpm/min for 5 min[36] and the supernatant was stored at -80 ℃.

### 2.4 NA activity assay

NA activity was assayed with MU-NANA as a substrate.[37] The supernatant of chicken egg embryonic allantoic fluid were first dissolved in pH 6.5 MES buffer (32.5 mM), which contains 4 mM calcium chloride. For NA activity inhibition assay, 49 μL of the supernatant was incubated with 1 μL DMSO dissolved TCM compound at different concentrations at 37 ℃ for 30 min in a black 96-well ELISA plate. Then 50 μL of 20 μM MU-NANA were added. TCM compounds with or without 20 μM MU-NANA were also detected the fluorescence intensity as control. Fluorescence intensity was measured using the FLX800 fluorescence microplate reader (Bio-Tek) with excitation wavelength at 360 nm and emission wave length at 450 nm. The detection lasted for 8 min. The fluorescence intensity changing rate of was determined as the NA activity. The level of inhibition was determined by the initial rates of the reaction with or without the compounds added. The median inhibitory concentration ($IC_{50}$) was defined as the concentration of detected compounds to reduce the NA activity by 50% relative to the reaction mixture containing NA without compounds.

### 2.5 Median Tissue culture infective dose ($TCID_{50}$) determination

MDCK cells were cultivated in DMEM and re-plated 2 days before infection in 96 wells plates. Serial 10-fold dilutions of the allantonic fluid (H1N1 or H3N2) were prepared, then the diluted fluid was added in MDCK cells which contain 10,000 cells per well to incubate for 2 h for virus to infect. The media for dilution was DMEM supplemented with 1 μg/mL TPCK-treated trypsin. Treated MDCK cells were washed 3 times by DMEM and cultured in DMEM with TPCK-treated trypsin (1 μg/mL) for 24 h. 24 h later, MDCK cells were washed 3 times and cultured in DMEM with 2% FBS. After 3 days, MTT assay was used to determinate the virus-induced cytopathic effect (CPE), which indicated the presence of virus, $TCID_{50}$ was calculated by the Reed-Muench method.

### 2.6 Cytotoxicity assay

MTT assay was also used to determinate the cytotoxic effects of natural compounds on MDCK cells. MDCK cells were grown in 96 wells plate in DMEM with 10% FBS and subsequently incubated with concentration gradient of compounds for 24 h at 37 ℃. Cell viability was detected by 15 μL MTT (5 mg/ml) in 100 μL DMEM for 4 h and measured the absorbance with spectrophotometer at 570 nm. The half-maximum cytotoxic concentration ($CC_{50}$) was defined as the concentration which reduced the 50% $OD_{570}$ of treated cells to untreated cells.

### 2.7 Viral growth inhibition assay

To detect the antiviral effect of the samples on influenza virus (H1N1 and H3N2), MDCK cells were grown in DMEM medium supplemented with 10% FBS and antibiotics. For the assay, MDCK cells were seeded into 96-well culture plates at a density of $3\times10^3$ per well and incubated for 24 h until 75%~85% confluency. Monolayer MDCK cells were washed with DMEM medium twice. There are two types of treatment: 1. We used 200 μL aliquot of virus which is at the optimal dose (100 $TCID_{50}$) mixed with 200 μL concentration gradient of compounds for 2 h at 37℃. The mixture was added into the wells to infect the MDCK cells. 2 h later, the virus-infected MDCK cells were washed with DMEM medium three times and cultured with DMEM medium with trypsin (1 μg/mL) and after 24 h, DMEM which contained the 2% FBS was changed ； 2. We used 200 μL aliquot of virus at the optimal dose for 2 h at 37 ℃ in medium without serum. The virus-infected MDCK cells were washed with DMEM medium three times and added different concentrations of compounds for 2 h.[26] The cells in the absence of compound without or with virus added were used as control.

For both types of treatment, 2 h later, MDCK cells were also washed with DMEM medium three times and cultured with DMEM medium with trypsin (1 μg/mL) and after 24 h, DMEM which contained the 2% FBS was changed. Following 3 days incubation, the monolayers were examined for CPE. For the CPE, the monolayers were washed to remove dead cells and debris, MTT assay was used to evaluate the antiviral effect of the anti-NA compounds on influenza virus. Concentration for 50% of maximal effect ($EC_{50}$) was defined as the concentration of detected compounds to enhance the cell viability by 50% between the cell viability of cells infected influenza virus without compounds and the cell viability of cells with no infection.

After 3 days of incubation, the cells contained cell-associated virus and extracellular virus with DMEM culture solution were frozen and unfrozen 3 times to rupture the cells. Then the solution was centrifuged with 2000 rpm for 5 min.[38] The supernatant was transferred, and the quantity of virus was represented by the NA activity. 50 μL of supernatant was added into black 96-well ELISA plate and 50 μL of 20 μM MU-NANA were also added, the rest of operation was carried out as described above. The solution in the absence of compound with virus was used as control.

**2.8 The inhibition type of SA on the activity of NA**

To determinate the type of inhibition of NA by SA, we performed enzyme kinetics with NAs from influenza virus (H1N1 and H3N2). In NA activity assay, we used 50 μL allantonic fluid which contain of NA of influenza virus (H1N1 or H3N2) as the control and added 100, 150 or 200 μM SA respectively, the mixtures were added into a black elisa plate and incubated at 37 ℃ for 30 min. Then 50 μL MU-NANA substrate solution which concentration were 0.5, 1, 1.5, 2 nmol were added into the control or the experiment wells. The fluorescence intensity measured as mentioned in NA activity assay. Based on the reciprocal concentration (X) and the reciprocal fluorescence intensity (Y), the double-reciprocal plot was obtained.

**2.9 Molecular docking simulation**

To study the interaction and the conformation of the protein-ligand complex, SA was docked into the N1, N2 NA protein using the AutoDock 4.0 program based on Lamarkian Genetic Algorithm (Scripps Research Institute, La Jolla, CA).[39] Due to the lack formation of NA which we used, the crystal structure of N1, N2 which are highly homology (PDB ID: 3TI6_A and PDB ID: 4GZP_A) were obtained from the RCSB Protein Data Bank (http://www.rcsb.org/pdb). The structure of oseltamivir (Fig. 1A) was obtained from PubChem (CID: 65028). The structure of SA (Fig. 1B) was obtained from PubChem (CID: 6443665). The predicted complexes were optimized and ranked according to the empirical scoring function, ScreenScore, which estimated the binding free energy of the ligand receptor complex. Each docking was performed twice, and each operation screened 250 conformations for the protein-ligand complex that were advantageous for docking; each docking had 500 preferred conformations. The most stable conformation distinguished which had the minimal binding energy was shown by Discovery Studio (DS) 3.5 Visualizer.

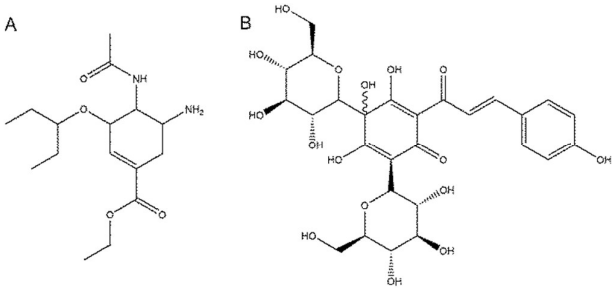


**Figure 1.** Chemical structures of compounds. (A) Oseltamivir; (B) Safflomin A (SA).

**2.10 Drug synergism studies**

To analyze the drug synergism on the effect of treatment of NA activities of N1 and N2 with SA and the oseltamivir, alone or in combination, isobologram analysis were used, according to the results by CalcuSyn Windows software (Biosoft, Cambridge, United Kingdom) for dose-effect analysis and synergism/antagonism quantification.[40] The conservative isobologram assumes that two drugs have independent or dissimilar modes of actions.[41] For two-drug combination design, the combination of the drugs at their equipotent ratio (the ratio of their $IC_{50}$s) was chosen. A mixture of the two drugs was prepared and the mixture was serially diluted (2-fold dilutions, SA: oseltamivir carboxylate is equal to 1:1, 0.5:1 and 0.25:1 at the concentration of their $IC_{50}$ values) to obtain a wide dosage range, as indicated in the CalcuSyn standard protocol. For single-drug treatment, serial dilutions were prepared from the serial dilutions of 0.1-0.5 times and 1-4 times of each compound's $IC_{50}$ value, using the same protocol. 30 μL of dissolved NAs were added into a 96-black plate. After NAs were added, 10 μL of SA at the concentration mentioned above of was added and 10 μL of the oseltamivir carboxylate in the different proportional concentrations were added at 37 °C for 30 min, each concentration was repeated 3 times. Then 50 μL of 20 μM MU-NANA substrate solution was added. The fluorescence intensity was detected same as the NA activity assay.

Dose inhibition curves were drawn for SA and oseltamivir carboxylate, used alone or in combination. The $IC_{50}$ values were plotted against the fractional concentrations of oseltamivir carboxylate and SA on the x axis and y axis, respectively. The evaluation of drug synergism based on a median-effect equation has been widely used. Using the median-effect equation, dose-effect curves for each drug and combination of drugs were generated and the combination index (CI) were calculated. To determinate the interactions between SA and oseltamivir carboxylate, CI was calculated. CI analysis provides qualitative information on the drug interaction. Its value calculated as described in equation A.

$$\mathbf{CI} = \frac{C_{A,x}}{IC_{x,A}} + \frac{C_{B,x}}{IC_{x,B}} \qquad \text{(A)}$$

CA,x and CB,x represent the concentrations of drug SA and drug oseltamivir carboxylate used in combination to achieve x% single drug effect. ICx,A and ICx,B are the concentrations for single drug to achieve the same effect.

For two-drug combinations, in the isobologram plot, if the combination data point falls on the diagonal, an additive effect is indicated; if it falls on the lower left, synergism is indicated, whereas if it falls on the upper right, antagonism is indicated. A CI of >1 denotes antagonism, a CI equal to 1 denotes additivity, and a CI of <1 denotes synergism. In particular, CI values in the range of 0.1 to 0.3, 0.3 to 0.7, and 0.7 to 0.85 are considered to indicate strong synergism, synergism, and moderate synergism, respectively.

**2.11 Statistical analysis**

The results were expressed as mean±S.E.M. for three independent experiments.

## Results

**3.1 SA inhibit the NA activities of influenza virus**

NA is the most effective drug target for influenza virus. There are numbers of herbal medicines used to treat influenza viral infection in traditional Chinese medicinal clinics, however, the compounds that could inhibit NA activity in these herbs have not been systematically tested. We used a natural compound library of 289 compounds which derived from TCMs to screen their NA inhibitory activities. First, NA of HIN1 virus was used in the NA activity assay and each compound was tested once. A representative result was shown in Fig. 2. An inhibition of the NA activity was detected when the fluorescent intensity of the product in the presence of the compound was lower than the control reaction. Then, we used selected compounds (as marked in Fig. 2) which showed inhibitory activity toward the NA of H1N1 to detect $IC_{50}$ values of NAs for H1N1 and H3N2 of type A and type B influenza virus. The $IC_{50}$ values were shown in Table 1. In order to eliminate the false positive caused by the natural compound, the fluorencese intensity of selected compounds with or without 20 μM MU-NANA were also detected. No influence on the fluorencese intensity in the presence of these compounds with or without substrate was observed. One compound, SA, showed inhibitory activities toward these NAs. The $IC_{50}$ values were 143.80±9.13, 155.33±17.37, and 104.72±8.91 μM toward NAs for H1N1 and H3N2 of type A and type B influenza virus, respectively.

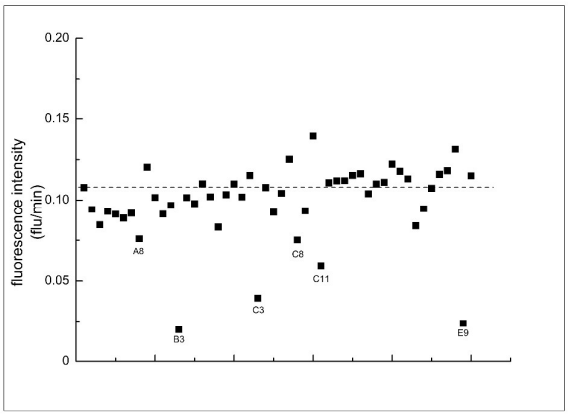


**Figure 2.** Screening of NA (H1N1) inhibitors using compounds in Plate δ. 49 μL NA derived from H1N1 were mixed with 1 μL compound at 37 ℃ for 30 min. 50 μL 20 μM MU-NANA substrate solution was added to detect fluorescence intensity. Imaginary line represented the fluorescence intensity of N1 without compounds. Compounds marked position were detected one which has effective to inhibit N1.

Table 1. Selected compound's $IC_{50}$ for H1N1, H3N2 and B in Plate δ.

| Well No. in Plate δ | $IC_{50}$ Value towards NA of Influenza Virus H1N1 (μM) | $IC_{50}$ Value towards NA of Influenza Virus H3N2 (μM) | $IC_{50}$ Value towards NA of type B Influenza Virus (μM) |
|---|---|---|---|
| A8 | ≥200 | —— | ≥200 |
| B3 | 164.53±4.05 | ≥200 | 136.51±16.20 |
| C3 | 143.80±9.13 | 155.33±17.37 | 104.72±8.91 |
| C8 | ≥200 | —— | ≥200 |
| C11 | ≥200 | —— | ≥200 |
| E9 | ≥200 | ≥200 | ≥200 |

**3.2 Inhibition of influenza A virus growth in MDCK cells by the SA**

Since SA showed anti-NA activities, we then tested whether it could protect cells from viral infection. We first examined the effect of SA on the cell viability. MDCK cells were used in the assay with concentration gradient of SA (from 100 to 500 μM). Half-maximum cytotoxic concentration ($CC_{50}$) of SA after 24h exposure of MDCK cells to it were shown in Fig. 3 and the $CC_{50}$ is 414.12±12.58 μM. This result showed that SA had minimal cytotoxicity in low concentrations.

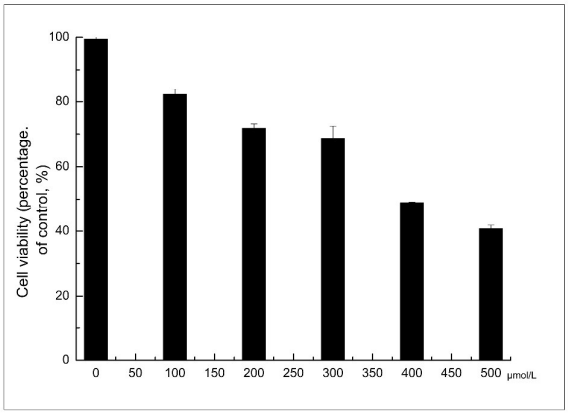


**Figure 3.** MTT assay was performed to evaluate the cytotoxic effects of SA on MDCK cells. MDCK cells were grown with 0, 100, 200, 300, 400 and 500 μM SA for 24h at 37 ℃. Then added 150 μL of MTT in DMEM, incubating for 4h and measuring the absorbance at 570 nm. Each point represents the mean±S.E.M. for three independent experiments.

In the presence of the virus, the MDCK cells viability was reduced. To determine the median tissue culture infective dose ($TCID_{50}$) of H1N1 or H3N2, MDCK cells were cultivated in DMEM and a serial 10-fold dilutions of the allantonic fluid (containing H1N1 or H3N2) were added for virus to infect. Three days after infection, MTT assay was used to determinate the virus-induced cytopathic effect (CPE), and $TCID_{50}$ was calculated by the Reed-Muench method. The $TCID_{50}$ values were $10^{-4.2}$ (H1N1) and $10^{-7.5}$ (H3N2), respectively.

To determine the anti-viral activity of SA, the MDCK cells were infected 100 $TCID_{50}$ of virus. Compared with control which has no influenza virus infection, the cell viability was greatly reduced when the MDCK cells were infected with 100 $TCID_{50}$ of virus, which indicated the H1N1 virus caused severe damage to the MDCK cells (Fig. 4a). To determinate whether the SA protected the MDCK cells from the infection of H1N1 influenza virus, we used two types of treatments. As mentioned in the methods section, SA was added to the MDCK cells upon or post viral infection. The results demonstrated that under both conditions, SA protected MDCK cells from viral damage, the protecting effects increased with the increase of the compound concentration (Fig. 4a). The $EC_{50}$ of SA measured is 82.36±11.74 μM for the viral infected MDCK cells (Table 2). Thus in agreement with that SA inhibited NA activities, the compound could reduce cell damage caused by influenza virus infection.

We also used H3N2 virus to infect the MDCK cells in the same way as the H1N1 virus (Fig. 4b). The results were similar to H1N1 virus infected MDCK cells. The $EC_{50}$ of SA measured is 160.33±2.06 μM for the viral infected MDCK cells (Table 2).

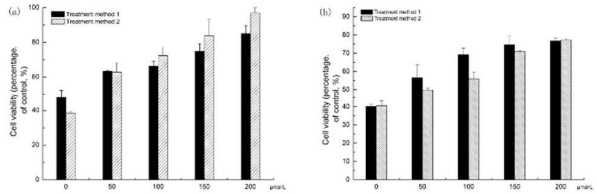


**Figure 4.** SA protected MDCK cells from viral infection. To detect the antiviral effect of SA on H1N1 (a) and H3N2 (b), we used two treatment methods as described in materials and methods: Method 1, influenza virus (H1N1 or H3N2) at 100 $TCID_{50}$ were mixed with concentration gradient of SA for 2h before applied to the MDCK cells. Method 2, influenza virus at 100 $TCID_{50}$ were added into MDCK cells, 2h later, cells were washed and SA was added. MDCK cells were infected with influenza virus (H1N1 or H3N2) and 0, 50, 100, 150, 200 μM of SA were used in the treatment. Each point represents the mean±S.E.M. for three independent experiments.

Table 2. The calculation of Saffomin A to treat influenza virus.

| $IC_{50}$(μM) | | | $CC_{50}$ (μM) | $EC_{50}$ (μM) | |
|---|---|---|---|---|---|
| H1N1 | H3N2 | B | | H1N1 | H3N2 |
| 143.80± 9.13 | 155.33± 8.91 | 104.72± 8.91 | 414.12± 12.58 | 82.36± 11.74 | 160.33 ±2.06 |

The results of cell viability indicated that SA could protect the MDCK cells from viral damage. Nonetheless, it did not show whether SA suppress the viral replication in MDCK cells. As viral numbers could be represented by the NA activities they carry, we measured the NA activity which reflect the multiplication of virus.[42] The NA activities in MDCK cells infected the H1N1 and H3N2 without SA was regarded as 100%. When SA were added with an increased concentration, the cellular NA activities were reduced in both treatment methods against H1N1 or H3N2. Which represented the inhibition of the viral reproduction (Fig. 5). The results also showed that SA reduced the virus yield in MDCK cells in a dose-dependent manner and it were consistent with the results of CPE assay.

**Figure 5.** Inhibitroy effects of SA on influenza virus yield in

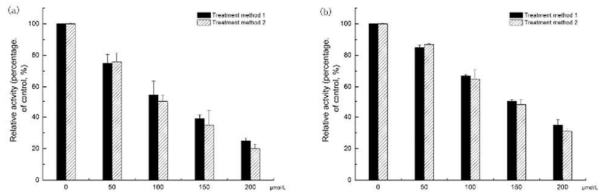


MDCK cells. MDCK cells were cultured with virus at different concentrations of SA as described in materials and methods. Cell culture supernatants collected and detected for H1N1 virus yield (a) and H3N2 yield (b) by measured NA activity. Virus yield expressed as percent NA activity of culture supernatants of SA-free with virus infected cells. Each point represents the mean±S.E.M. for three independent experiments.

**3.3 The inhibition type of SA on the activity of NA**

The inhibition kinetics of NA by SA were studied. Under the experimental conditions employed, the reaction of NA with SA followed Michaelis-Menten kinetics. The double-reciprocal plots of the enzyme inhibited by SA were shown in Fig. 6a (H1N1) and Fig. 6b (H3N2). The results showed that the plots of 1/v versus 1/[S] gave straight lines with different slopes, and the lines intersected at one point on the X-axis. These results suggested that the types of inhibition by SA were noncompetitive. It indicated that SA interacts with NA in a site other than the catalytic center, and this interaction may change the conformation of the NA active site and in turn reduce the activity of NA.

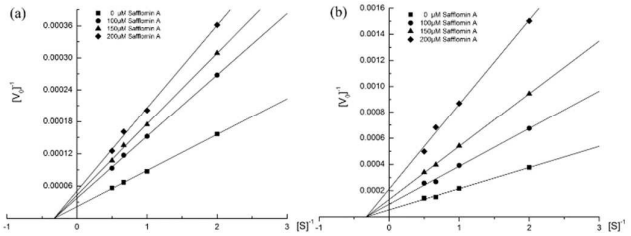


**Figure 6.** To determinate which type of SA inhibit to the NA of N1 (a) and N2 (b), we used two types of NA with 100,150 and 200 μM SA and added substrate sloution (final concentration is 0.5, 1, 1.5, 2 nmol). Based on the reciprocal concentration (X) and the reciprocal fluorescence inthensity (Y), the double-reciprocal plot was obtained.

### 3.4 SA bind to non-catalytic site of NA by molecular docking

To study the possible interaction sites of SA and the NAs, we used molecular simulation analysis. The crystal structure of N1, N2 were obtained from the RCSB Protein Data Bank and SA was docked into the N1 or N2 NA protein using the AutoDock 4.0 program based on Lamarkian Genetic Algorithm as described in materials and methods. Our docking results showed that SA bound in the non-catalytic site of N1 and N2, which is different from the control drug, oseltamivir carboxylate. Oseltamivir docked to the center of the active site of N1 and N2. Meanwhile, SA bound at the backside of N1 or N2 (Fig. 7). Fig. 8 showed the details of the compound-NAs complexes. Notably, the locations where SA bound to N1 and N2 were different. The residues His409-Leu412 of N1 formed an alpha helix structure, which was the absent in N2 (Fig. 8). Such structural differences created a deep groove on N2 surface for SA to bind (Fig. 7 black circle).

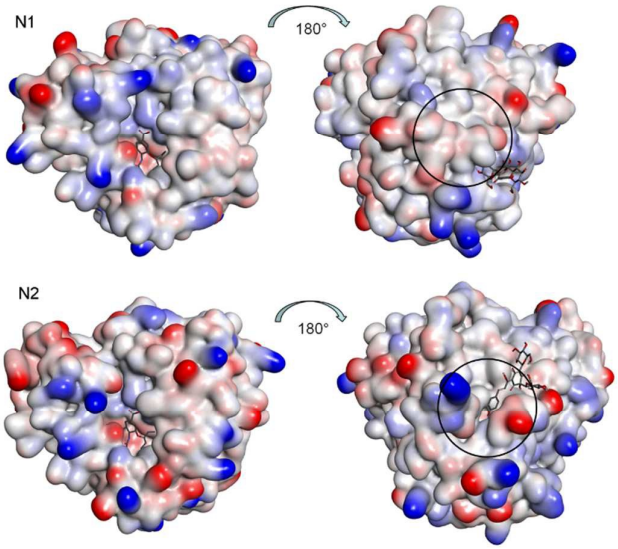


**Figure 7.** Schematic drawing of interrelation between inhibitors and NAs by protein contact potential of vacuum electrostations. Blue represents positive charge, red represents negative charge. Inhibitors are oseltamivir (left) and SA (right), showed by stick. Carbon skeleton of inhibitors were painted grey. Oseltamivir located in the center of the active site of NAs, SA bound at the backside of NAs.

To identify the binding forces contributed to the compound-NAs complexes, the estimated free energy of binding, which including the Van der Waals energy, electrostatic energy, H-bond energy, dissolving energy, final total internal energy, torsional free energy, and unbound system's energy, were calculated. The values of the estimated free energy of binding for SA with NAs shown in Table 3 were consistent with the experimental values: the inhibition constant of SA to N1 (143.80±9.13 μM) were lower than to N2 (155.33±8.91 μM), and the calculated free energy of binding for SA with NAs were -6.19 kcal/mol for N1 and -5.66 kcal/mol for N2.

Table 3. The Estimated Free Energy of Binding, $IC_{50}$ of SA with NAs.

| NAs | Enery (kcal/mol) | $IC_{50}$ (μM) |
|---|---|---|
| N1 | -6.19 | 143.80±9.13 |
| N2 | -5.66 | 155.33±8.91 |

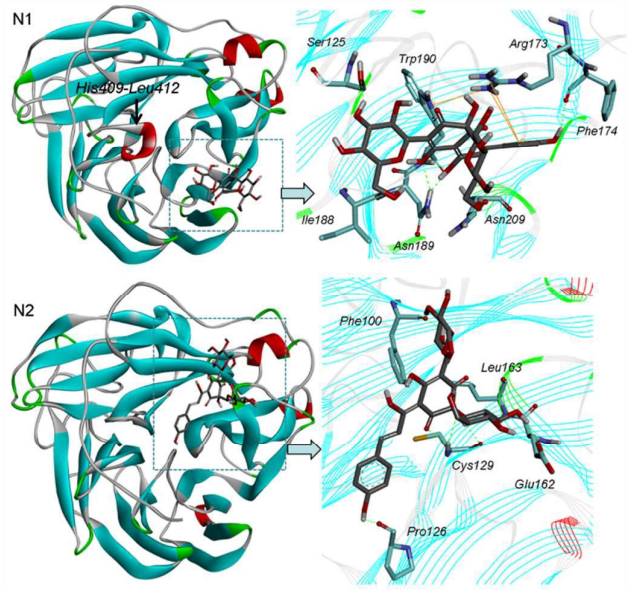


**Figure 8.** Schematic drawing of interrelation between SA and NAs. NAs were showed by ribbon and SA showed by stick. Right figures were the details of square frame in the left figures. That is hydrogen bonds and pi-pi interaction formed between SA and NAs. Hydrogen bonds are shown by green dash line. Pi-pi interactions are shown by orange solid line.

Hydrogen bonds formed between compound and protein were usually contributed to the stability of the substrate-enzyme complexes, and more hydrogen bonds form a more stable complex. In the present study, the compound-NAs complexes models were visualized by DS4.0 molecular graphics system. Our results shown that SA formed eight hydrogen bonds with both N1 (Fig. 9A) and N2 (Fig. 9B), respectively. From analyzing the hydrogen bonds interaction, some critical NAs residues were identified (Table 4, 5). The residues of Ser125, Phe174, Ile188, Asn189, Trp190 and Asn209 of N1 were considered to be important in the interaction. Meanwhile, the presence of five residues, Phe100, Pro126, Cys129, Glu162 and Leu163, were previously identified as conserved residues in SA-N2 interaction.

SA bound to N1 not only by hydrogen bond interaction, but also by a strong conjugation effect (Fig. 9). Normal conjugated effect, also known as pi-pi interaction, was due to the formation of conjugated Pi bond caused by the effect of the molecular nature of the charge. By analyzing the pi-pi interaction results (Table 6), Arg173 of N1 was identified to be important amino acids in the pi-pi interaction.

Table 4. Hydrogen bond interaction parameters for SA and N1 residues.

| Donors Atom | Receptors Atom | Distances(Å) |
|---|---|---|
| Asn189: HD21 | SA: O12 | 2.12 |
| Asn189: HD21 | SA: O15 | 2.26 |
| Trp190: HN | SA: O15 | 1.70 |
| Asn209: HD22 | SA: O13 | 2.04 |
| SA: H66 | Asn209: OD1 | 2.08 |
| SA: H67 | Ile188: O | 2.22 |
| SA: H63 | Ser125: OG | 1.91 |
| SA: H75 | Phe174: O | 2.14 |

Table 5. Hydrogen bond interaction parameters for SA and N2 residues.

| Donors Atom | Receptors Atom | Distances(Å) |
|---|---|---|
| Cys129: HN | SA: O11 | 1.91 |
| Cys129: HN | SA: O3 | 2.42 |
| Leu163: HN | SA: O4 | 2.17 |
| SA: H56 | Cys129: O | 2.13 |
| SA: H60 | Glu162: OE1 | 1.75 |
| SA: H63 | Phe100: O | 1.90 |
| SA: H62 | Phe100: O | 1.97 |
| SA: H75 | Pro126: O | 2.13 |

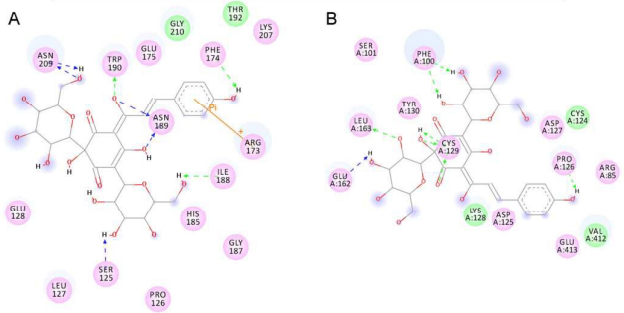


**Figure 9.** The binding patterns between inhibitors and NAs. (A) N1, (B) N2. Hydrogen-bond interactions with amino acid main chains are represented by a green dashed arrow directed towards the electron donor. Hydrogen-bond interactions with amino acid side-chains are represented by a blue dashed arrow directed towards the electron donor. Pi interactions are represented by an orange solid line with symbols indicating the interaction. Residues involved in hydrogen-bond, charge or polar interactions are represented by pink circles. Residues involved in van der Waals interactions are represented by green circles. The solvent accessible surface of an interacting residue is represented by a blue halo around the residue. The diameter of the circle is proportional to the solvent accessible surface.

By analyzing the estimated free energy of binding, hydrogen bonds interaction and pi-pi interaction, we consider that SA has a strong binding effect with N1 than N2.

Table 6. Pi-pi interaction parameters for each SA and N1 residues.

| End1 | End2 | Distances(Å) |
|---|---|---|
| SA | N1:Arg173 | 5.08 |
| SA | N1:Arg173 | 6.78 |

### 3.5 SA and oseltamivir act synergistically against N1 and N2

Oseltamivir carboxylate is widely used in the clinics for the treatment of influenza. It is well know as a potent competitive inhibitor for NA. Since SA inhibit noncompetitively of NA, it is of great interest to know if these two drugs can act synergistically. NAs were mixed with SA and oseltamivir carboxylate to detect the rate of inhibition. The effect of inhibitory rate on SA and oseltamivir carboxylate in combination against N1 and N2 were shown in Fig. 10. The SA-oseltamivir carboxylate combination treatment was significantly more effective than when used alone.

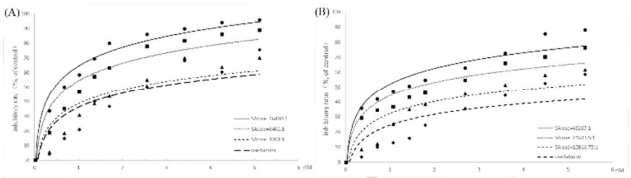

**Figure 10.** The effect of inhibitory rate on SA and oseltamivir in combination against N1 (A) and N2 (B). For two-drug combination design, the combination of the drugs at their equipotent ratio (the ratio of their IC50s) was chosen. A mixture of the two drugs was prepared and the mixture was serially diluted (2-fold dilutions, SA: oseltamivir carboxylate is equal to 1:1, 0.5:1 and 0.25:1 at the concentration of their IC50 values) to obtain a wide dosage range, as indicated in the CalcuSyn standard protocol. For single-drug treatment, serial dilutions were prepared from the serial dilutions of 0.1-0.5 times and 1-4 times of each compound, using the same protocol.30 μL of dissolved NAs were added into a 96-black plate. After NAs were added, the concentration mentioned above of 10 μL SA was added and 10 μL the oseltamivir carboxylate in the different proportional concentrations were added at 37 °C for 30 min, each concentration repeated 3 times. Then 50 μL of 20 μM MU-NANA substrate solution was added. The fluorescence intensity was detected as the NA activity assay.

To further analyze the synergistic effect of the two drugs, a log dose-effect curve and median-effect plot were generated for both drugs using the CalcuSyn software (Fig. 11A). The x intercept of the median-effect plot determines the median-effect dose (Dm), which, under the conditions described, is equivalent to the $IC_{50}$ values of the drug; the Dm were found to 140.89 μM and 2.42 nM for SA and oseltamivir carboxylate against N1, respectively, when administered separately. The Dm values of the two drug were 18 μM and 1.07 nM for SA and oseltamivir against N1, respectively, when the drugs are used in combination, indicating that the doses needed to achieve 50% inhibitory of N1 were approximately 7.8-fold and 2.26-fold lower than those needed in monotherapy for SA and oseltamivir carboxylate, respectively.

We also detected the effect of SA and oseltamivir carboxylate against N2 (Fig. 11B). The Dm values were 144.07 μM and 4.248 nM for SA and oseltamivir carboxylate against N2, respectively, when administered separately. However, the Dm values of the two-drug combination were 45.437 μM and 1.05 nM for SA and oseltamivir carboxylate against N2, respectively, when the drugs are used in combination, indicating the doses needed to achieve 50% inhibitory N2 were approximately 3.17-fold and 4.05-fold lower than those needed in monotherapy for SA and oseltamivir carboxylate, respectively (Fig. 11B).

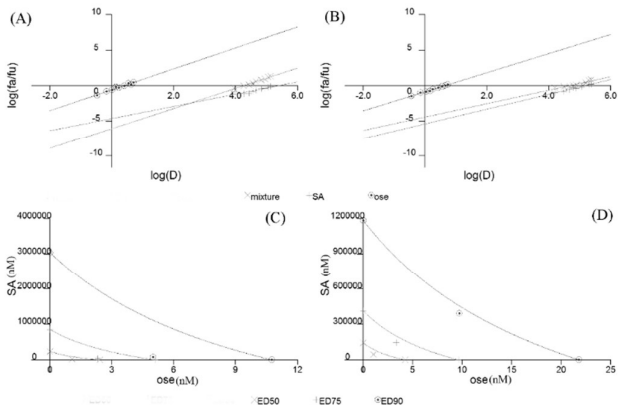


**Figure 11.** Analysis of the SA-oseltamivir combination treatment in NA of H1N1 and H3N2 under single-step and multistep. The treatment was the same as the effect of inhibitory rate on SA and oseltamivir carboxylate in combination against N1 and N2. (A) and (B), Median-effect curve plots for SA (SA), oseltamivir carboxylate (ose), and the combinatin of the two drugs (SA/ose) against N1 and N2, respectively, were generated with the CalcuSyn software (Fa, affected fraction; Fu, unaffected fraction; D, concentration of drug used). (C) and (D), Conservative isobologram plots of the combination of SA and ose against N1 and N2, respectively. Dose inhibition curves were drawn for SA and oseltamivir carboxylate, used alone or in combination. For each drug, equipoent combination of various doses (ED50, ED75, ED90 values) were determined using the CalcuSyn software and were plotted against the fractional concentrations of SA and ose on the y and x axis, respectively. Combination index (CI) values, represented by points below the lines, indicate synergy.

The evaluation of drug synergism based on a median-effect equation has been widely used. CalcuSyn-generated isobolograms based on the two drugs administered in combination at fixed ratios toward N1 and N2 are shown in Fig. 11C and D. The ED50, ED75, and ED90 (50%, 75%, and 90% equipotent doses) plots for each drug ratio fell below the line indicating a synergistic effect of the drug combination on NA activities. CI values were calculated for all conditions (Table 7). Under the used concentrations, the SA-oseltamivir carboxylate combination treatment was synergistic against both N1 and N2, with CI values ranging between 0.49 and 0.52 for N1, and CI values ranging between 0.56 and 0.88 for N2, respectively (Table 7). The CI values are consistent with conservative iosbologram plots.

Table 7. Effect of SA-oseltamivir combination treatments in N1 and N2 activities.

| | CI at indicated ED | | |
|---|---|---|---|
| | ED50 | ED75 | ED90 |
| H1N1 | 0.52 | 0.50 | 0.49 |

| | | | |
|---|---|---|---|
| H3N2 | 0.56 | 0.70 | 0.88 |

## Discussion

In this study, we tested 289 natural compounds for their inhibitory activities towards NAs of influenza virus. The NAs in the allantoic fluid of H1N1, and H3N2 of type A virus and type B virus were used in the assay. Among these compounds, we found that SA exhibited inhibitory activities to these NAs (Table 1). However, the $IC_{50}$ values were different toward these NAs, which was mostly possible due to difference of the residues and structure at the active site of the influenza virus NAs.

Next, we tested the viral inhibitory activity of the NA inhibiting compound SA in H1N1 or H3N2 infected MDCK cells. Although higher concentration of SA caused a reduction in the cell viability (Fig. 3), it also reduced CPE caused by influenza virus in MDCK cells in a dose-dependent manner (Fig. 4 and Fig. 5). These results suggest that SA could inhibit viral growth and protect cells from viral induced CPE by NA inhibition. Based on the structural characteristics of the NAs, type A influenza were divided into group-1 (comprising N1, N4, N5, N8) and group-2 (comprising N2, N3, N6, N7, N9). Our results also suggest that SA may reduce cell damage caused by either group-1 or group-2 type A influenza virus.

We also investigated the type of inhibition caused by SA with N1 or N2. According to the results shown in Fig. 6, SA inhibits NAs by a noncompetitive fashion. Molecular docking results were consistent with the enzyme kinetic analysis (Fig. 7). From analyzing the hydrogen bonds interaction, the residues of Ser125, Phe174, Ile188, Asn189, Trp190 and Asn209 of N1 were considered to be important (Table 4), and Phe100, Pro126, Cys129, Glu162 and Leu163 were identified as key residues in SA-N2 interaction (Table 5).

Traditional Chinese medicines (TCMs) have a long history in China to treat influenza. In the past, researchers found some TCMs to treat influenza. Heartleaf houttuynia herb (*Houttuynia cordata* Thunb.) was found to inhibit MDCK cell apoptosis induced by H3N2 virus.[43] *Asiatic toddalia* root (*Toddalia asiatica* Lam.) showed potent antiviral activities against H1N1 virus, with a 50% effective concentration valued of 4.7 mg/L in the MTS assay and 0.9 mg/L in the quantitative PCR assay.[44] Pu *et al*. used extractive from *Hypericum perforatum* known as a TCM for anti-bacteria and defervescence against H1N1 virus in *vivo* and *vitro*, they found that it could inhibit the H1N1 in MDCK cells with an $EC_{50}$ value of 40 μg/ml.[45] Despite a number of reports showed that TCMs could be inhibit influenza virus, limited effective compounds in TCMs were reported. As a consequence, the anti-influenza mechanisms for these TCMs were not known. In recent years, researchers have started to detect compounds in TCMs in cells or in animal models. A variety of polyphenols, flavonoids, saponins, glucosides and alkaloids isolated from TCMs have been studied and tested for anti-influenza activity. Hayashi *et al*. showed the inhibitory effect of trans-cinnamaldehyde (CA), one of the principal constituents of essential oil derived from *cinnamomi cortex*, on the growth of influenza A virus in *vitro* and in *vivo*, they found CA inhibit the influenza growth in dose-dependent manner and it could also inhibit the viral protein synthesis.[46] Four diarylheptanoids from the seed of *Alpinia katsumadai* showed NA inhibitory activities in micromolar range in *vitro* against H1N1. Katsumadain A which inhibit the NA of H1N1 with $IC_{50}$ value between 0.9 and 1.64 μM was also a constituent from the seed of *Alpinia katsumadai*.[43]

Dao *et al*. found 4 chalcone derived compounds from *Cleistocalyx operculatus* exhibited stronger NA inhibitory activities than flavanones, dihydroflavonols and isoflavones. These 4 chalcones had inhibitory effect against NAs from the wild-type and oseltamivir-resistant H1N1 influenza virus (H274Y mutant). The 4 chalcones inhibited N1 in noncompetitive manner and they could protect MDCK cells with a strong protective effect for viral infection and low toxicity to the host MDCK cells.[47] In another report, they found 8 chalcone derived compounds from *Glycyrrhiza inflata* could inhibit NA of influenza virus (H1N1 and H9N2). The 8 chalcones were all noncompetitive inhibitions.[48] SA is a chalcone glycoside. Our results showed that SA inhibited N1 and N2 in a noncompetitive manner. We determined the binding site of SA using molecular simulation (Fig. 8), and the result is in agreement with enzyme kinetics.

Some recent studies showed that the inhibitory effect of the anti-influenza drug bind to the catalytic site could be enhanced by another compound binding in the non-catalytic site. For example, the inhibition of on NAs (H9N2, H1N1, and NA mutants) by oseltamivir in the prescence of ehinantin binding with NA in a non-catalytic site was strengthened by several folds.[46] Because of binding in non-catalytic site, it is likely that SA may have potential to enhance the inhibitory effect of oseltamivir carboxylate against the oseltamivir-resistant mutant.

In contrast to the widely developed anti-influenza drugs, SA interact with NA at a non-catalytic site and it inhibit NA in micromolar range. It protects cell from viral damage and hinders virus replication in *vitro*. A synergistic antiviral effect was acquired when SA was administered in combination with oseltamivir carboxylate againt the neuraminidase activities of N1 and N2 (Fig. 10). Median-effect curves and conservative isobologram analysis also indicated that the SA-oseltamivir carboxylate combination treatment was synergistic, with CI values in the 0.49-0.52 against N1 and 0.56-0.88 against N2 (Fig. 11). Chalcones have been reported to inhibit NA of H1N1, in a noncompetitive manner and enhance the inhibitory effect of oseltamivir.[48] SA is a chalcone glycoside derivative. Oseltamivir located in the center of the active site of NAs while SA bound at the backside of NAs (Fig. 7). The different binding to the NA resulted different mode of action. It is most likely that the SA binding caused a change of NA conformation, which lead to a reduced activity of NA and a more efficient inhibition of NA by oseltamivir, thus resulted as synergism of inhibition. SA and oseltamivir carboxylate combination treatment were both synergistic against N1 and N2.



 

These findings suggest that SA exerts synergistic antiviral activity when using in combination with oseltamivir against NAs of H1N1 and H3N2. It is worthwhile to further test whether the synergism of SA and oseltamivir can overcome the drug resistance caused by the NA mutations and investigate the treatment strategy to add SA to oseltamivir as effective anti-influenza therapeutics.

## Conclusions

We identified SA from a Chinese medicinal herbal compound library as one of neuraminidase inhibitor. It showed a significant reduction for viral replication in MDCK cells against H1N1 and H3N2 influenza virus. The type of inhibition between SA and N1 or N2 was noncompetitive by the enzyme kineitc tests. The interaction of SA with N1 and N2 was simulated through molecular simulation and docking, which showed that SA bound in the non-active site of N1 and N2. Combination therapy studies were undertaken to investigate the effect of SA when administered in combination with oseltamivir. The results showed that SA-oseltamivir combination treatment resulted in synergism against N1 or N2. These results suggest that an herbal formulation containing SA may serve as an effective supplementary strategy to currently available anti-influenza therapeutics.

## Acknowledgements

The authors gratefully acknowledge financial support from the National Natural Science Foundation of China (No. 31170742 and No. 31370742) and Fund from Science and Technology Department of Jilin Province (No. 20130206066YY).

## Appendix

| ID No. | Name | Molecular weight |
|---|---|---|
| 110759 | Bornyl Acetate | 196.286 |
| 110776 | Venillic Acid | 168.147 |
| 11688 | Natural borneol | 154.249 |
| 111512 | Isoborneol | 154.249 |
| 110881 | Borneol | 154.2 |
| 110809 | Protocatechuic Acid | 154.12 |
| 100815 | Curcumol | 236.35 |
| 110728 | Menthol | 198.302 |
| 110845 | Salicylic Acid | 138.121 |
| 110792 | Butyl-phydroxybenzoate | 216.209 |
| 110831 | Gallic acid1 | 70.12 |
| 110747 | Camphor | 152.233 |
| 110885 | Caffeic Acid | 180.157 |
| 111735 | Liquidambaric acid | 440.65 |
| 100528 | Guaifenesin | 198.216 |
| 110808 | Catalnol | 362.329 |
| 111541 | Fumaric acid | 116.072 |
| 110810 | Protocatechuic aldehyde | 179.5 |
| 110812 | E-10-hydroxy-3-decylennic acide | 186.25 |
| 110708 | Paeonol | 166.174 |
| 110755 | Ursodeoxycholic Acid | 392.572 |
| 110851 | β-sitosterol | 414 |
| 110816 | Sodium Taurousodeoxycholate | 392.58 |
| 110815 | Sodium Taurocholate | 537.686 |
| 110806 | Chenodesoxuchalic Acid | 392.572 |
| 110803 | Cinobufagin | 442.545 |
| 110744 | Sarsasapogenin | 416.636 |
| 110846 | Sodium taurochenodeoxycholic | 522.694 |
| 110724 | Deoxycholic acid | 392.572 |
| 110718 | Recibufogenin | 384.508 |
| 111638 | Ecdysterone | 480.634 |
| 111731 | Fraxetin | 208 |
| 109711 | Columbianadin | 328.36 |
| 110741 | Aesculetin | 178.142 |
| 110837 | Isofraxidin | 222.194 |
| 110822 | Osthol | 244.29 |
| 110900 | Daphnetin | 178.142 |
| 110826 | Imperatorin | 270.28 |
| 110827 | Isoimperatorin | 270.28 |
| 111511 | Scoparone | 206.195 |
| 42096 | 6,7-dimethoxyl-coumarin | 206.19 |
| 110723 | Glycyrrhetinic acid | 470.64 |
| 110738 | Isopsoralen | 186.16 |
| 111513 | 7-methoxy coumarin | 176.17 |
| 111741 | 6-Hydroxy-7-methoxycoumarin | 192 |
| 111711 | Praeruptorin A | 386 |
| 110836 | Sesamine | 354.353 |
| 110835 | Ethyl-p-methoxycinnamate | 206.238 |
| 111568 | Linderane | 260.285 |
| 110854 | Dehydroandrographolide | 332.434 |
| 110797 | Andrographolide | 350.449 |
| 110865 | Bilobalide | 326.299 |
| 111747 | Protopanaxadiol | 460.6 |
| 111655 | Andrographolidi natril bisulfis | 262.13 |
| 110701 | Panaxadiol | 460.732 |
| 111664 | Epifriedelanol | 428.733 |
| 111525 | Dehydrocostuslactone | 230.302 |
| 110760 | Alantolactone | 232.318 |
| 110800 | Evodin | 470.512 |
| 110702 | Panaxatriol | 476.731 |
| 100200 | Artesunate | 384.43 |
| 110761 | Isoalantolactone | 232.318 |
| 110863 | Ginkgolide B | 424.399 |
| 110862 | Ginkgolide A | 408.399 |
| 110864 | Ginkgolide C | 440.398 |
| 1566 | Triptolide | 360.401 |
| 111665 | Germacrone | 218.335 |
| 111518 | Cucurbitacin IIa | 574.702 |
| 110742 | Ursolic acide | 456.7 |
| 110753 | Chlorogenic Acid | 354.309 |
| 110880 | Pseudolaric acid | 430.491 |
| 100271 | Artemether | 298.375 |
| 111663 | Friedelin | 426.717 |
| 111517 | Gossypol | 518.554 |
| 111581 | Shionone | 426.717 |
| 1539 | Diosgenin | 414.621 |
| 110709 | Oleanolic Acid | 456.7 |
| 111524 | Costunolide | 232.33 |

| | | | | | |
|---|---|---|---|---|---|
| 110787 | Aloin | 418.394 | 100080 | Rutin | 664.563 |
| 111575 | Polydatin | 390.384 | 110703 | Ginsenoside RgI | 1602.03 |
| 110794 | Rhaponticin | 420.41 | 110749 | Geniposide | 388.366 |
| 1110893 | Madecassicside | 975.121 | 110715 | Baicalin | 446.361 |
| 111582 | Cynanchagenin | 500.584 | 110721 | Hesperidin | 610.561 |
| 110887 | Uridine | 244.201 | 110734 | Jujuboside A | 1207.35 |
| 111574 | Syringin | 372.367 | 111573 | Typhaneoside | 770.685 |
| 111590 | Chonglou Saponin I | 855.021 | 110722 | Naringin | 580.535 |
| 110892 | Asiaticoside | 959.122 | 110740 | Ginsenoside Rb1 | 1109.29 |
| 111536 | Tubeimiside I | 1319.43 | 110804 | Ginsenoside Rg3 | 785.013 |
| 110819 | Arctiin | 534.552 | 111668 | Rhamnosylvitexin | 578.519 |
| 111571 | Isorhamnetin-3-O-nehesperidin | 624.56 | 110737 | Icariin | 676.662 |
| 110745 | Notoginsenoside R1 | 919.101 | 111521 | Hyperoside | 464.376 |
| 111523 | 5-o-Methyl visammioside | 452.453 | 110842 | Scutellarin | 492.473 |
| 111685 | Asperosaponin VI | 636.856 | 110879 | Adenosine | 267.242 |
| 110820 | Amygdalin | 457.429 | 111508 | D-Xylose | 150.13 |
| 110841 | Pseuoginsenoside F11 | 801.013 | 111506 | Arabinose | 150.131 |
| 111640 | Loganin | 390.382 | 110833 | Glucose anhydrous | 180.16 |
| 111515 | Stevioside | 804.872 | 111504 | D-Fructose | 180.156 |
| 110844 | 2,3,5,4'-tetrahedroxystilbene -2-O-D-glucoside | 406.383 | 111507 | Sucrose | 342.296 |
| | | | 110795 | Aloe-emodin | 270.237 |
| 111538 | Quercitroside | 448.377 | 110758 | Physcion | 284.263 |
| 111522 | prim-O-glucosylcimifugin | 468.451 | 110756 | Emodin | 270.237 |
| 111528 | Buddleoside | 592.55 | 110829 | 1,9-Dihydroxyanthraquinone | 240.211 |
| 111553 | Ginserg Stem and Leaf Faponins | -- | 110769 | Shikonin | 288.295 |
| 110778 | Saikosaponin D | 780.982 | 110852 | Cryptonshinone | 296.36 |
| 110770 | Gentiopicrin | 356.325 | 111605 | Sulfotanshinone Sodium | 396 |
| 110777 | Saikosaponin A | 780.982 | 110796 | Chrysophanol | 254.237 |
| 110736 | Paeoniflorin | 480.462 | 110766 | Tanshinonel IIA | 702.616 |
| 111530 | Acteoside | 624.587 | 110867 | Tanshinonel I | 294.34 |
| 110785 | Swertiamain | 374.34 | 100228 | Menadiol Acetate | 258.269 |
| 111610 | Liguiritin | 418.394 | 110884 | Mollugin | 284.307 |
| 110821 | Forsythin | 534.552 | 110757 | Rhein | 284.22 |
| 110818 | Salidroside | 300.304 | 111514 | Wogonin | 284.263 |
| 110781 | Astragaloside | 784.97 | 110856 | Silymarin | 482.436 |
| 110782 | Clinodiside A | 959.125 | 110762 | Alpinetin | 270.28 |
| 110754 | Ginsenoside Re | 947.154 | 111502 | Daidzein | 254.237 |
| 111580 | Methyl Hesperidin | 624.587 | 111554 | Vitexicarpin | 374.3 |
| 111592 | Chonglou Saponin VI | 738.906 | 111595 | Baicalein | 270.237 |
| 110870 | Sanqi total Saponins | 872.0 | 111555 | Lysionotin | 344.315 |
| 111537 | Pinoresinol diglucoside | 682.67 | 110860 | Isorhanetin | 316.262 |
| 110891 | Huangshanyao Saponins Extract | -- | 110861 | Kaempferol | 286.236 |
| 111596 | Picroside-II | 512.461 | 111557 | Irisflorentin | 386.352 |
| 111607 | Mangiferin | 422.34 | 110850 | Farrerol | 300.306 |
| 111695 | Sophoricoside | 432.37 | 100081 | Quercetin | 302.236 |
| 111670 | Echinacoside | 786 | 110752 | Puerarin | 416.378 |
| 111714 | Sec-o-glucosylhamaudol | 438 | 110763 | Cardamonin | 270.28 |
| 111745 | Picfeltrarraenin IA | 762.9 | 110772 | Patchoulialcohol | 222.366 |
| 111748 | Ginsenoside Rh2 | 622.6 | 111701 | Chrysin | 254 |
| 111742 | Sweroside 358. | 34 | 111520 | Luteolin | 286.23 |
| 111727 | Picroside I | 492 | 110872 | Arginine | 174.201 |
| 111738 | Daidzin | 416 | 111578 | L-Hydroxyproline | 131.13 |
| 111719 | Ginsenoside Rf | 801 | 110735 | Glycine | 75.067 |
| 111686 | Ginsenoside Rb3 | 1079 | 110875 | L-Citrulline | 175.186 |
| 111629 | 2"-O-galloylhyperin | 616.48 | 110890 | Histidine | 155.155 |
| 110871 | Sanqi Stem and Leaf Saponins | -- | 110876 | Leucine | 131.173 |
| 111593 | Chonglou Saponin VII | 1049.2 | 110873 | DL-Aminopropionic Acid | 89.09 |

| | | |
|---|---|---|
| 110889 | Threomine | 119.18 |
| 110874 | DL-Aminovaleic Acid | 117.15 |
| 111533 | Homoharringtonine | 545.621 |
| 110779 | Papaverine Hydrochloride | 375.846 |
| 100747 | Vincamine | 354.443 |
| 110894 | Betaine | 117.146 |
| 111666 | Dihydrocapsaicin | 307.428 |
| 110886 | Adenine | 135.127 |
| 110775 | Piperine | 285.338 |
| 110784 | Sophoridine | 248.364 |
| 110780 | Oxymatrine | 264.363 |
| 100249 | Raceanisodamine | 305.38 |
| 110805 | Matrine | 248.364 |
| 100121 | Theophylline | 180.164 |
| 100243 | Huperzine A | 258.316 |
| 110774 | Sinomenine | 329.39 |
| 100526 | Hydroxycamptothecin | 364.352 |
| 110801 | Rutaecarpine | 287.315 |
| 100476 | Methscopolamine bromide | 398.292 |
| 111654 | Dictamnine | 199.205 |
| 111652 | Oxysophocarpine | 262.347 |
| 110802 | Evodiamine | 303.358 |
| 100382 | Paclitaxel | 853.906 |
| 110733 | Jatrorrhizine Hydrochloride | 374.887 |
| 111718 | Chelerythrine | 348.36 |
| 111651 | Cavidine | 353.412 |
| 111647 | Cepharanthin | 606.707 |
| 100270 | Nimodipine | 418.44 |
| 100336 | Tinidazole | 247.273 |
| 110839 | Capsaici | 305.412 |
| 100135 | Glibenclamide | 494.004 |
| 100412 | Sulfagunidine | 232.26 |
| 110732 | Palmatine Hydrochloride | 391.888 |
| 110717 | Indirabin | 262.263 |
| 100547 | Lappaconitine Adhewsive | 584.7 |
| 110746 | Aristolochic acide A | 341.272 |
| 11071 | Indigotin | 262.27 |
| 110726 | Tetrahydropalmatine | 355.428 |
| 110895 | Bullatine A | 343.503 |
| 100250 | Isosorbide Dinitrate | 236.136 |
| 110750 | Peimine | 431.651 |
| 110751 | Peinine | 429.64 |
| 111667 | Dehydrocavidine | 353 |
| 110711 | Tetrandrine | 622.75 |
| 110793 | Fangchinoline | 608.723 |
| 110720 | Aconitine | 645.737 |
| 110883 | Trigonelline | 137.136 |
| 111566 | Nuciferine | 295.376 |
| 110712 | Stachydrine Hydrochloride | 179.644 |
| 110853 | Protopine | 353.369 |
| 100465 | Methylcantharidinimde | 209 |
| 111608 | Convza Blinii Extract | -- |
| 111501 | Allantoin | 158.116 |
| 110807 | Gastrodin | 286.278 |
| 110704 | Cordycepin | 251.242 |
| 110866 | Ginkgo Biloba Extract | -- |
| 100385 | Hilieidum | 284.26 |
| 110877 | Catechin | 290.268 |
| 110843 | Diphenyl | 154 |
| 110878 | Epicatechin | 290.268 |
| 110811 | Dracohodin perochlorate | 366.75 |
| 110896 | Succinic Acide | 118.088 |
| 110817 | Chuangxiongzine Hydrochlorid | 208.69 |
| 100247 | Sodium Houttuyfonate | 302.36 |
| 100845 | Ligustrazine Phosphate | 242 |
| 110855 | Sodium Danshensu | 220 |
| 110857 | Schisandrin | 432.5 |
| 110859 | Hupehenine | 415.345 |
| 110888 | Cycloyirobuxinum D | 402.364 |
| 111535 | Resveratrol | 390 |
| 111637 | Safflomin A | 612.533 |
| 111689 | β,β-Dimethylacrylalkannin | 370.39 |
| 111696 | Liensinine perchlorate | 610.74 |
| 111699 | Galangin | 270.25 |
| 111700 | Fraxinellon | 232 |
| 111702 | Sinapine cyanide sulfonate | 368 |
| 111703 | Formonontin | 268.27 |
| 111712 | RaddeaninA | 896 |
| 111717 | 1,3-O-dicaffeoylquinic acid | 516.45 |
| 111721 | Oridonin | 364.43 |
| 111744 | 1-Hydroxy-3,4,5-trimethoxyxanthone | 302 |
| 110765 | γ-Schisandrin | 400.46 |
| 110764 | Deoxyschizandrin | 416.507 |
| 110882 | Magnoshinin | 414.491 |
| 110773 | Ferulic Acid | 194.18 |
| 111532 | Bergenin | 328.271 |
| 111645 | Podophyllotoxin | 414.405 |
| 111529 | Schisantherin | 536.57 |
| 111660 | Loureirin A | 286.322 |
| 111558 | Loureirin B | 316.35 |
| 111539 | Toddalolatone | 308.326 |
| 110729 | Magnolol | 266.334 |
| 110730 | Honokiol | 266.334 |
| 111561 | Fargesin | 370.396 |
| 100202 | Artemisinin | 282.332 |
| 111559 | Cochinchinenin C | 514.566 |
| 110823 | Curcumin | 368.38 |
| 111594 | Total ginkgolic acid | 346.49 |

## Notes and references

1 Centers for Disease Control and Prevention, MMWR Early release, 2009, 58, 1-54.
2 K. R. Short, P. C. Reading, L. E. Brown, J. Pedersen, B. Gilbertson, E. R. Job, K. M. Edenborough, M. N. Habets, r. A. Zome, P. W. Hermans, D. A. Diavatopoulos and O. L. Wijburg, Infect Immun, 2013, 81, 645-652.
3 R. Gao, B. Cao, Y. Hu, Z. Feng, D. Wang, W. Hu, J. Chen, Z. Jie, H. Qiu, K. Xu, X. Xu, H. Lu, W. Zhu, Z. Gao, N. Xiang, Y. Shen, Z. He, Y. Gu, Z. Zhang, Y. Yang, X. Zhao, L. Zhou, X. Li, S. Zou, Y. Zhang, X. Li, L. Yang, J. Guo, J. Dong, Q. Li, L. Dong, Y. Zhu, T. Bai, S. Wang, P. Hao, W. Yang, Y. Zhang, J. Han, H. Yu, D. Li, G. F. Gao, G. Wu, Y. Wang, Z. Yuan and Y. Shu, The New England journal of medicine, 2013, 368, 1888-1897.

4 N. L. La Gruta, K. Kedzierska, J. Stambas and P. C. Doherty, Immunology and cell biology, 2007, 85, 85-92.
5 H. N. Gao, H. Z. Lu, B. Cao, B. Du, H. Shang, J. H. Gan, S. H. Lu, Y. D. Yang, Q. Fang, Y. Z. Shen, X. M. Xi, Q. Gu, X. M. Zhou, H. P. Qu, Z. Yan, F. M. Li, W. Zhao, Z. C. Gao, G. F. Wang, L. X. Ruan, W. H. Wang, J. Ye, H. F. Cao, X. W. Li, W. H. Zhang, X. C. Fang, J. He, W. F. Liang, J. Xie, M. Zeng, X. Z. Wu, J. Li, Q. Xia, Z. C. Jin, Q. Chen, C. Tang, Z. Y. Zhang, B. M. Hou, Z. X. Feng, J. F. Sheng, N. S. Zhong and L. J. Li, The New England journal of medicine, 2013, 368, 2277-2285.
6 Q. Li, L. Zhou, M. Zhou, Z. Chen, F. Li, H. Wu, N. Xiang, E. Chen, F. Tang and D. Wang, New England Journal of Medicine, 2013.
7 X. Wang, W. Jia, A. Zhao and X. Wang, Phytotherapy research : PTR, 2006, 20, 335-341.
8 R. J. Russell, L. F. Haire, D. J. Stevens, P. J. Collins, Y. P. Lin, G. M. Blackburn, A. J. Hay, S. J. Gamblin and J. J. Skehel, Nature, 2006, 443, 45-49.
9 T. Betakova, Curr Pharm Des, 2007, 13, 3231-3235.
10 M. N. Matrosovich, T. Y. Matrosovich, T. Gray, N. A. Roberts and H.-D. Klenk, Journal of virology, 2004, 78, 12665-12667.Das K., Aramini J. M., Ma L. C., Krug R. M. and Arnold E., Nature Structural & Molecular Biology, 2010, 17, 530-538.
11 L. M. Surhone, M. T. Timpledon and S. F. Marseken, Rimantadine, Betascript Publishing, 2010.
12 P. K. Cheng, A. P. To, T. W. Leung, P. C. Leung, C. W. Lee and W. W. Lim, Emerging infectious diseases, 2010, 16, 155.
13 A. C. Hurt, J. Ernest, Y. M. Deng, P. Iannello, T. G. Besselaar, C. Birch, P. Buchy, M. Chittaganpitch, S. C. Chiu, D. Dwyer, A. Guigon, B. Harrower, I. P. Kei, T. Kok, C. Lin, K. McPhie, A. Mohd, R. Olveda, T. Panayotou, W. Rawlinson, L. Scott, D. Smith, H. D'Souza, N. Komadina, R. Shaw, A. Kelso and I. G. Barr, Antiviral Res, 2009, 83, 90-93.
14 J. Boon-Long, K. Ikuta, G.-R. Bai and N. Takeda, Bulletin of the Department of Medical Sciences, 2014, 55, 117-127.
15 G. Orozovic, K. Orozovic, J. D. Jarhult and B. Olsen, PLoS One, 2014, 9, e89306.
16 A. Meijer, A. Lackenby, O. Hungnes, B. Lina, S. Van Der Werf, B. Schweiger, M. Opp, J. Paget, J. van de Kassteele and A. Hay, Emerging infectious diseases, 2009, 15, 552.
17 M. Samson, A. Pizzorno, Y. Abed and G. Boivin, Antiviral Res, 2013, 98, 174-185.
18 T. Baranovich, R. Saito, Y. Suzuki, H. Zaraket, C. Dapat, I. Caperig-Dapat, T. Oguma, I. I. Shabana, T. Saito and H. Suzuki, Journal of Clinical Virology, 2010, 47, 23-28.
19 V. P. Mishin, K. Sleeman, M. Levine, P. J. Carney, J. Stevens and L. V. Gubareva, Antiviral Res, 2014, 101, 93-96.
20 Q. Liu, J. Ma, D. R. Strayer, W. M. Mitchell, W. A. Carter, W. Ma and J. A. Richt, Expert Rev Anti Infect Ther, 2014, 12, 165-169.
21 J. Zhou, D. Wang, R. Gao, B. Zhao, J. Song, X. Qi, Y. Zhang, Y. Shi, L. Yang, W. Zhu, T. Bai, K. Qin, Y. Lan, S. Zou, J. Guo, J. Dong, L. Dong, Y. Zhang, H. Wei, X. Li, J. Lu, L. Liu, X. Zhao, X. Li, W. Huang, L. Wen, H. Bo, L. Xin, Y. Chen, C. Xu, Y. Pei, Y. Yang, X. Zhang, S. Wang, Z. Feng, J. Han, W. Yang, G. F. Gao, G. Wu, D. Li, Y. Wang and Y. Shu, Nature, 2013, 499, 500-503.
22 R. Hai, M. Schmolke, V. H. Leyva-Grado, R. R. Thangavel, I. Margine, E. L. Jaffe, F. Krammer, A. Solorzano, A. Garcia-Sastre, P. Palese and N. M. Bouvier, Nature Communications, 2013, 4.
23 K. Sleeman, V. M. Mishin VPDeyde, Y. Furuta, A. I. Klimov and L. V. Gubareva, Antimicrobial Agents & Chemotherapy, 2010, 54, 2517-2524.
24 K. Das, J. M. Aramini, L. C. Ma, R. M. Krug and E. Arnold, Nature Structural & Molecular Biology, 2010, 17, 530-538.
25 A. Dias, D. Bouvier, T. Crépin, A. A. Mccarthy, D. J. Hart, F. Baudin, S. Cusack and R. W. H. Ruigrok, Nature, 2009, 458, 914-918 (916 April 2009) | doi :2010.1038/nature07745.
26 L. Tian, Z. Wang, H. Wu, S. Wang, Y. Wang, Y. Wang, J. Xu, L. Wang, F. Qi and M. Fang, Journal of ethnopharmacology, 2011, 137, 534-542.
27 H. Ge, Y. F. Wang, J. Xu, Q. Gu, H. B. Liu, P. G. Xiao, J. Zhou, Y. Liu, Z. Yang and H. Su, Nat Prod Rep, 2010, 27, 1758-1780.
28 J. Y. Ho, H. W. Chang, C. F. Lin, C. J. Liu, C. F. Hsieh and J. T. Horng, Viruses, 2014, 6, 1861-1875.
29 N. Oyuntsetseg, M. A. Khasnatinov, P. Molor-Erdene, J. Oyunbileg, A. V. Liapunov, G. A. Danchinova, S. Oldokh, J. Baigalmaa and C. Chimedragchaa, BMC Complement Altern Med, 2014, 14, 235.
30 X. Wang, X. Xu, Y. Li, X. Li, W. Tao, B. Li, Y. Wang and L. Yang, Integrative biology : quantitative biosciences from nano to macro, 2013, 5, 351-371.
31 D. A. Gschwend, A. C. Good and I. D. Kuntz, Journal of molecular recognition : JMR, 1996, 9, 175-186.
32 J. H. An, D. C. W. Lee, A. H. Y. Law, C. L. H. Yang, L. L. M. Poon, A. S. Y. Lau and S. J. M. Jones, Journal Of Medicinal Chemistry, 2009, 52, 2667-2672.
33 U. S. Tambunan, A. A. Parikesit, Y. Dephinto and F. R. Sipahutar, Acta Pharm, 2014, 64, 157-172.
34 Natural Products Database (NPD) http://wiki.compbio.ucsf.edu/wiki/index/php/Natural_products_database. 2011.
35 Y. Wang, D. Wu, D. Yu, Z. Wang, L. Tian, Y. Wang, W. Han and X. Fang, J Mol Model, 2012, 18, 3445-3453.
36 P. Ramanujam, W. Tan, S. Nathan and K. Yusoff, Archives of virology, 2002, 147, 981-993.
37 M. Potier, L. Mameli, M. Belisle, L. Dallaire and S. B. Melancon, Anal Biochem, 1979, 94, 287-296.
38 D. F. Smee, J. H. Huffman, A. C. Morrison, D. L. Barnard and R. W. Sidwell, Antimicrob Agents Chemother., 2001, 45, : 743–748.
39 G. M. Morris, D. S. Goodsell, R. S. Halliday, R. Huey, W. E. Hart, R. K. Belew and A. J. Olson, Journal of computational chemistry, 1998, 19, 1639-1662.
40 Chou TC, Hayball M and L. CW., CalcuSyn-windows software for dose-effect analysis and synergism/antagonism quantification, and user's manual., Biosoft, Cambridge, United Kingdom, 1996.
41 T. C. Chou and P. Talalay, European Journal of Biochemistry, 1981, 115, 207-216.
42 N. DP and R. U., J Virol Methods, 2004, 122, 9–15.
43 U. Grienke, M. Schmidtke, J. Kirchmair, K. Pfarr, P. Wutzler, R. Dürrwald, G. Wolber, K. R. Liedl, H. Stuppner and J. M. Rollinger, Journal of medicinal chemistry, 2009, 53, 778-786.
44 S. Lu, Y. Qiao, P. Xiao and X. Tan, Zhongguo Zhong yao za zhi= Zhongguo zhongyao zazhi= China journal of Chinese materia medica, 2005, 30, 998-1001.
45 X.-y. Pu, J.-p. Liang, X.-h. Wang, T. Xu, L.-y. Hua, R.-f. Shang, Y. Liu and Y.-m. Xing, Virologica Sinica, 2009, 24, 19-27.
46 K. Hayashi, N. Imanishi, Y. Kashiwayama, A. Kawano, K. Terasawa, Y. Shimada and H. Ochiai, Antiviral Res, 2007, 74, 1-8.
47 T. T. Dao, B. T. Tung, P. H. Nguyen, P. T. Thuong, S. S. Yoo, E. H. Kim, S. K. Kim and W. K. Oh, Journal Of Natural Products, 2010, 73, 1636-1642.
48 T. T. Dao, P. H. Nguyen, H. S. Lee, E. Kim, J. Park, S. I. Lim and W. K. Oh, Bioorganic & medicinal chemistry letters, 2011, 21, 294-298.